Sensors and Actuators B 163 (2012) 90–96

Contents lists available at SciVerse ScienceDirect

Sensors and Actuators B: Chemical

journal homepage: www.elsevier.com/locate/snb

On-line fingerprinting of fluids using coaxial stub resonator technology

N.A. Hoog-Antonyuk[a,c,*], W. Olthuis[a], M.J.J. Mayer[b], D. Yntema[c], H. Miedema[c], A. van den Berg[a]

[a] BIOS – The Lab-on-a-Chip Group, MESA+ Institute of Nanotechnology, University of Twente, P.O. Box 217, 7500 AE Enschede, The Netherlands
[b] EasyMeasure B.V., Breestraat 22, 3811 BJ Amersfoort, The Netherlands
[c] Wetsus, Agora 1, Leeuwarden 8900CC, The Netherlands

ARTICLE INFO

Article history:
Received 5 July 2011
Received in revised form 4 January 2012
Accepted 5 January 2012
Available online 14 January 2012

Keywords:
Dielectric permittivity measurements
Coaxial sensor
Coaxial stub resonator
Water quality

ABSTRACT

Here we demonstrate the proof-of-principle of a coaxial stub resonator to assess the dielectric properties of fluids. This radio-frequency spectroscopy method is based on coaxial stub technology and comprises quarter wave length open-ended resonators that are filled with a liquid sample as dielectric between inner and outer conductor. Changes in the dielectric properties of the liquid sample result in changes in the electric properties of the resonator, e.g., its resonance frequency and quality factor. In addition to a batch resonator, results obtained with a flow-through resonator indicate that the concept can be further developed into a cost-efficient and low-maintenance sensor for the on-line fingerprinting of the dielectric properties of fluids, such as drinking or waste water, ethanol and glycerol.

1. Introduction

In drinking water, surface water, waste water and industrial process fluids, a large number of toxic or otherwise undesired components can be present at a wide range of concentration levels. In order to safeguard water quality, the early detection of pollutants in water is mandatory. However, currently existing (bio) chemical detection methods are labor-intensive and by implication expensive. Even more important, all these methods are off-line providing a momentary signature only. The aim of the present study was to develop a fingerprinting sensing device that operates on-line instead and that is based on recording a physical rather than a (bio) chemical parameter representative for water quality.

Examples of physical parameters to monitor and track the composition of a fluid are those related to its dielectric properties, e.g., dielectric permittivity and loss tangent. This can be achieved by using high or microwave frequency techniques with capacitors or (coaxial) resonators as sensitive elements [1–10]. Both techniques will now be discussed briefly.

In a capacitance-based measurement, the capacitance (as a sensing element) can be connected to an inductor to create a resonant circuit with a characteristic resonant frequency. However, due to the high impedance of the capacitive element, the resonant frequency of the circuit is rather sensitive to errors caused not only by the finite resistance of the monitored liquid, but also, for instance, by the parasitic capacity of all elements forming the measuring circuit. As a result, the total capacitance of the system can be of the same order of magnitude as the parasitic capacitance of the measuring circuit, especially at high frequencies [11,12].

Microwave technology to determine the dielectric permittivity of a fluid is based on measuring the reflection coefficient at a defined reference plane, usually the one at the interface of the dielectric to be investigated. Advantages of these microwave based systems are a high resolution resulting from the high frequencies applied and a high absolute sensitivity [13,14].

Apart from these advantages, there are some disadvantages such as the complicated and, consequently, high construction costs, off-line sample analysis and, since the measurements are based upon reflection, the prerequisite that at the micro scale the test solution can be considered homogeneous [15,16]. Other studies assess dielectric properties of fluids in stub resonators through so-called scattering or *S*-parameter measurements requiring relatively expensive equipment [17–22]. Additionally, the interpretation of *S*-parameter models is less straight forward which complicates the analysis [23].

The present contribution deals with the feasibility of a quarter wave length open ended coaxial stub resonator as a flow-through and on-line sensing element for tracking changes in the dielectric properties of a fluid. The fluid is present as the dielectric between the inner and outer conductor of the resonator. This technique is less sensitive to errors as compared to the previously mentioned reflection techniques. On-line analysis is realized by pumping the sample continuously through the resonator using an inlet and outlet for the fluid to be investigated. Since the

* Corresponding author at: BIOS – The Lab-on-a-Chip Group, MESA+Institute of Nanotechnology, University of Twente, P.O. Box 217, 7500 AE Enschede, The Netherlands. Tel.: +31 631077502.
E-mail address: Natalia.Antonyuk@wetsus.nl (N.A. Hoog-Antonyuk).

0925-4005/$ – see front matter © 2012 Elsevier B.V. All rights reserved.
doi:10.1016/j.snb.2012.01.012

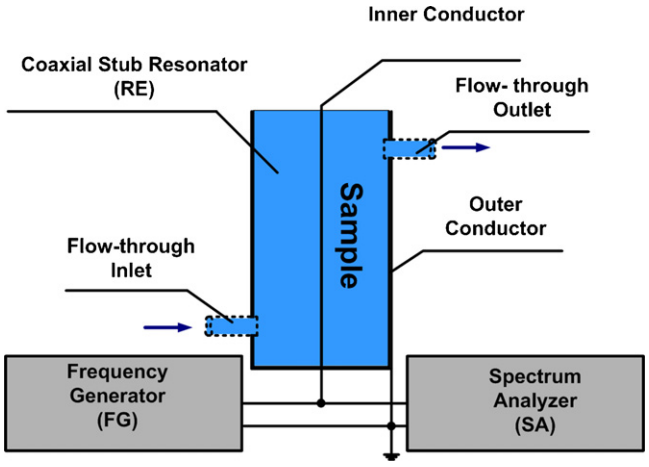

Fig. 1. Basic principle of the coaxial stub resonator sensing system consisting of a function generator (FG), a spectrum analyzer (SA) and the coaxial resonator (RE). The dotted structures indicate the inlet and the outlet of the flow-through resonator. Apart from lacking the in- and outlet, the design of the batch resonator is essentially the same.

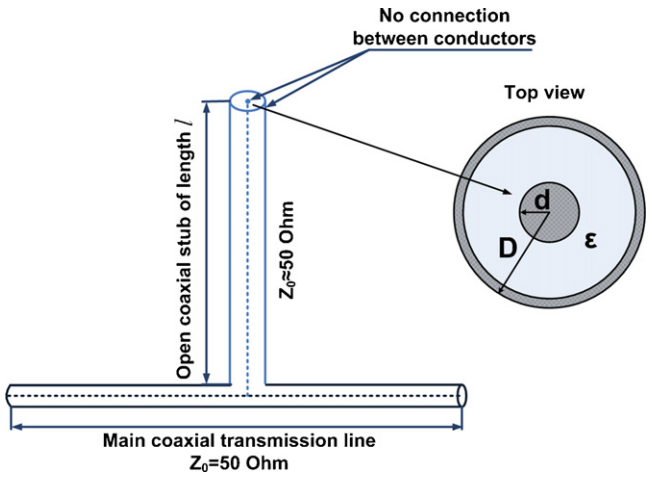

Fig. 2. The schematic representation of the open ended coaxial stub resonator of length l and its connection to the transmission line between function generator FG and spectrum analyzer SA. Z_0 is the characteristic impedance of the transmission line and of the coaxial stub. Note that the inner and outer conductors at the end of the coaxial stub are not connected. The inset shows a top view of the coaxial stub.

sensor system can be designed such that the fluid volume between inner and outer conductor is relatively large, it is envisaged that the sensor can also be applied for analysis of heterogeneous mixtures. In principle, the concept outlined here creates the possibility for on-line complex dielectric permittivity measurements in resonant circuits at high frequencies with a high quality factor, i.e., at radio frequencies between 3 and 30 MHz (HF), at frequencies in the range of 30–300 MHz (VHF) and at frequencies in the microwave range between 300 MHz and 300 GHz (both UHF and EHF) [24]. The on-line flow-through system enables fast, cost-efficient sample analyses.

2. Sensing technique

Fig. 1 gives a schematic overview of the coaxial resonator described in this study and its connection to the coaxial transmission line between the function generator (FG) and the spectrum analyzer (SA).

The sensing system comprises a function generator (FG), with an internal output resistance of $Z_s = 50\,\Omega$, connected to a spectrum analyzer (SA), with an internal input resistance of $Z_{SA} = 50\,\Omega$, both connected by a coaxial transmission line with a characteristic impedance of 50 Ω. To this coaxial transmission line, a quarter wave length open ended coaxial stub resonator (RE) is connected. The advantage of an open ended coaxial stub resonator over a closed ended one is that its base resonant frequency is a factor of 2 lower. As a result, the required length of the resonator can be reduced without compromising the frequency range of the response. The resonator consists of an inner conductor positioned in the center of a hollow outer conductor. The sample to be analyzed is present as dielectric between inner and outer conductor.

In addition to Fig. 1, Fig. 2 gives a detailed schematic overview of the coaxial stub resonator itself.

Fig. 3 shows the electrical equivalent circuit of the device shown in Figs. 1 and 2, with the quarter wave length coaxial stub resonator represented as a lumped element series resonant circuit. As shown and discussed later on, Fig. 3 presents an adequate circuit analog of our device for frequencies close to the base frequency of the resonator [25].

It is noted that a lumped element circuit as shown in Fig. 3 predicts one resonant frequency only, whether that is the first or one of the higher harmonics. In contrast, the coaxial sensing element records all harmonics within a defined frequency range. Even though the model used can be extended to account for these odd harmonics, using the Telegrapher's equations [26–30], such aim was considered beyond the scope of the present study.

The propagation velocity of electromagnetic waves is affected by the dielectric between the inner and outer conductor of the resonator [26–30]. Therefore, the resonant frequency (f_{res}) of a quarter wave length open ended coaxial resonator with effective length l is given by (1):

$$f_{res} = \frac{c \cdot (2n-1)}{4l\sqrt{\varepsilon_r \mu_r}} \quad (1)$$

where f_{res}, resonance frequency (Hz); c, speed of light in free space (m/s); l, length of coaxial resonator (m); μ_r, relative magnetic permeability; ε_r, relative dielectric permittivity; n, harmonic number.

By filling the resonator of Fig. 1 with a fluid sample, and making an amplitude versus frequency or A–f plot using the frequency generator and spectrum analyzer, the base resonant frequency as well its odd harmonics can be determined from the minimums in the plot. Substitution of the experimentally determined value of f_{res} and the stub resonator length l in Eq. (1) enables the calculation of the relative dielectric permittivity of the fluid sample assuming $\mu_r = 1$.

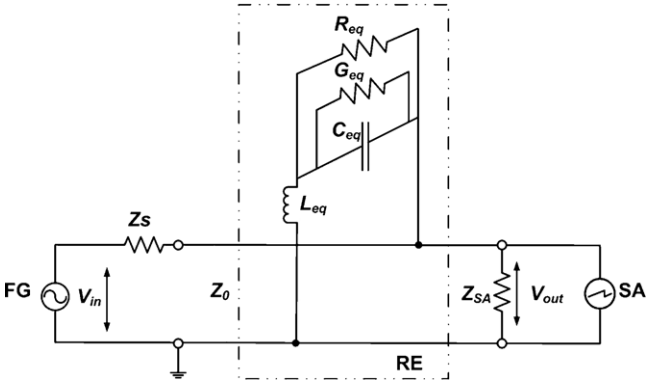

Fig. 3. The electrical equivalent circuit of the sensor system of Figs. 1 and 2. Parameters L_{eq}, C_{eq}, G_{eq} and R_{eq} represent the lumped element inductance of the resonator, the lumped element capacitance of the resonator, the conductivity of the dielectric and losses due to the skin effect in the inner and outer conductors of the coaxial resonator, respectively.

Besides the resonant frequency, the shape of the amplitude – versus – frequency (*A–f*) plot also provides information on the dielectric losses in the fluid between inner and outer conductor G_{eq} and on the skin effect in the inner and outer conductors R_{eq}. In order to quantify the values of G_{eq} and R_{eq} near the base resonant frequency of the stub resonator, the transfer function V_{out}/V_{in} needs to be derived.

The inductance (L'), series resistance (R'), capacitance (C') and dielectric conductance (G') of a coaxial transmission line (all expressed per unit length) are give by [26,31]:

$$L' = \frac{\mu_0\mu_r}{2\pi}\ln\left(\frac{D}{d}\right) + \frac{\mu_0\mu_r}{2\pi}\sqrt{\frac{\rho}{2\omega\mu_0\mu_r}}\left(\frac{1}{d}+\frac{1}{D}\right) \quad (2)$$

$$R' = \frac{R_s}{2\pi}\left(\frac{1}{D}+\frac{1}{d}\right) \quad (3)$$

$$C' = \frac{2\pi\varepsilon_0\varepsilon_r}{\ln(D/d)} \quad (4)$$

$$G' = \frac{2\pi\sigma}{\ln(D/d)} \quad (5)$$

where μ_0, magnetic permeability of free space (vacuum permeability) (H m^{-1}): $\mu_0 = 4\pi \times 10^{-7}$; ε_0, dielectric permittivity of free space (vacuum permittivity) (F m^{-1}): $\varepsilon_0 = 1/(\mu_0 \cdot c)^{-1/2}$; D, diameter of outer conductor (m); d, diameter of inner conductor (m); R_s, surface resistivity (Ω); ω, angular frequency, $\omega = 2\pi f$ (rad/s); ρ, specific resistance of the metal (Ω m); σ, conductance of the dielectric between inner conductor and outer conductor (S/m).For frequencies applied in this study ($f > 5$ MHz), the contribution of internal inductance to L' is negligible [26]. Hence, starting from Eq. (2), the following approximation holds (6):

$$L' \approx \frac{\mu_0\mu_r}{2\pi}\ln\left(\frac{D}{d}\right) \quad (6)$$

Note that this approximation turns L' into a frequency-independent parameter. The distributed parameters in Eqs. (3)–(6) can be related to the lumped element values L_{eq}, C_{eq}, G_{eq} and R_{eq} by comparing the general solution of the Telegrapher's equation for a quarter wavelength open ended coaxial stub with the solution for the lumped element model near the base resonant frequency f_{res} (7)–(10) [25]:

$$L_{eq} = L' \cdot \frac{l}{2} \quad (7)$$

$$C_{eq} = C' \cdot \frac{8l}{\pi^2} \quad (8)$$

$$G_{eq} = G' \cdot \frac{8l}{\pi^2} \quad (9)$$

$$R_{eq} = R' \cdot \frac{l}{2} \quad (10)$$

It is noted that the base resonant frequency of the quarter wave length coaxial stub can be derived directly from Eqs. (4), (6), (7) and (8) and the resonance criterion $LC = 1/(\omega^2)$, which results from Eq. (1) for $n = 1$.

For the transfer function, relating the voltage of the input signal supplied by the function generator V_{in} to the voltage of the output signal recorded by the spectrum analyzer V_{out}, the following relation is obtained (11):

$$\frac{V_{out}(\omega)}{V_{in}(\omega)} = \frac{1/((1/(j\omega L_{eq} + (1/(j\omega C_{eq} + G_{eq})) + R_{eq}) + (1/Z_{SA}))}{(Z_s + (1/(1/(j\omega L_{eq} + (1/(j\omega C_{eq} + G_{eq})) + R_{eq})) + (1/Z_{SA})))} \quad (11)$$

where V_{in}, voltage of the input signal supplied by FG (V); V_{out}, voltage of the output signal recorded by SA (V); Z_s, internal resistance of the frequency generator (Ω); Z_{SA}, internal resistance of the spectrum analyzer (Ω). For our fluid-filled coaxial stub resonator, the first step in the analysis to obtain the relative dielectric constant of the fluid is the determination of the resonant frequency of the *A–f* plot using Eq. (1). The experimentally observed shape of the *A–f* plot can be compared to model simulations using Eqs. (3)–(11). Since the *A–f* plot renders the value of the dielectric constant the only remaining unknown parameters in Eqs. (3)–(11) are the values of G_{eq} and R_{eq}.

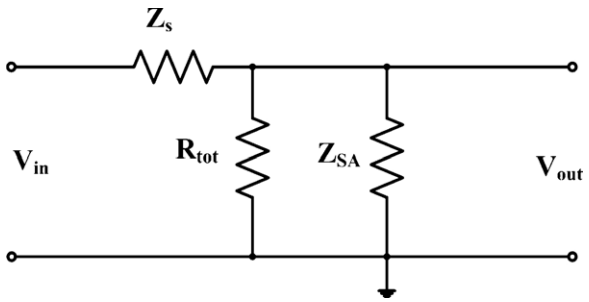

Fig. 4. Representation of the electrical equivalent circuit in Fig. 3 at resonance as a simple resistive voltage divider.

According to the lumped element circuit in Fig. 3, the total impedance Z_{tot} of the coaxial stub resonator is given by (12):

$$Z_{tot} = j\omega L_{eq} + \frac{1}{j\omega C_{eq} + G_{eq}} + R_{eq} \quad (12)$$

For the imaginary part of Z_{tot}, i.e., $Im(Z_{tot})$ the following expression can be derived (13):

$$\mathrm{Im}(Z_{tot}) = \frac{G_{eq}(G_{eq}\omega L_{eq} + \omega C_{eq}R_{eq}) - \omega C_{eq}(1 - \omega^2 L_{eq}C_{eq} + R_{eq}G_{eq})}{G_{eq}^2 + \omega^2 C_{eq}^2} \quad (13)$$

At resonance, with $\omega = \omega_{res}$ and $Im(Z_{tot}) = 0$, ω_{res} can be expressed in terms of L_{eq}, C_{eq} and G_{eq} (14):

$$\omega_{res} = \frac{1}{\sqrt{L_{eq}C_{eq}}}\sqrt{1 - G_{eq}^2\frac{L_{eq}}{C_{eq}}} \quad (14)$$

For $Re(Z_{tot})$, the following expression can be derived (15):

$$Re(Z_{tot}) = \frac{G_{eq}(1 - \omega^2 L_{eq}C_{eq} + R_{eq}G_{eq}) + \omega^2 C_{eq}(G_{eq}L_{eq} + C_{eq}R_{eq})}{G_{eq}^2 + \omega^2 C_{eq}^2} \quad (15)$$

Substitution of Eq. (14) into Eq. (15) provides the following expression for R_{tot} at resonance (16):

$$R_{tot} = R_{eq} + \frac{G_{eq}L_{eq}}{C_{eq}} \quad (16)$$

At resonance, the electrical equivalent circuit of Fig. 3 is reduced to a simple resistive voltage divider (Fig. 4). Since the internal impedance of both the function generator and the spectrum analyzer equals 50 Ω, the value of R_{tot} can be calculated from V_{out} and V_{in} at resonance by the use of Eq. (17).

$$R_{tot} = \frac{50 \cdot V_{out}}{V_{in} - 2 \cdot V_{out}} \quad (17)$$

R_{eq} in Eq. (16) represents the series resistance in the resonant circuit caused, predominantly, by the skin effect in inner and outer conductor. The value of R_{eq} can be determined using Eq. (18) after constructing a second coaxial stub resonator but filled with air as dielectric and resonating at the same resonant frequency as the one filled with fluid sample. It is noted that the coaxial stub resonator filled with air is longer than the one filled with fluid since the relative dielectric constant of the fluid is larger than that of air.Since

Table 1
The parameters of the flow-through and the batch resonators.

Parameters	Flow-through resonator	Batch resonator
Length, l	101.0 (cm)	34.0 (cm)
Inner conductor diameter, d	0.5 (mm)	0.5 (mm)
Inner diameter of the outer conductor, D	22.0 (mm)	22.0 (mm)
Diameters of the fluid inlet and outlet	7.0 (mm)	

the dielectric losses in air are negligible, i.e., $G_{eq} = 0$, the total resistance $R_{tot} = R_{eq}$. The skin effect is proportional to the length of inner and outer conductor of the resonator. Since the two resonators, one filled with air, the other with fluid, resonate at the same frequency but have different length, $R_{eq(fluid)}$ needs to be corrected for the resonator length according to:

$$R_{eq(fluid)} = R_{eq(air)} \cdot \frac{l_{(fluid)}}{l_{(air)}} \tag{18}$$

Once the value of $R_{eq(fluid)}$ has been determined, the single unknown parameter left in Eq. (16) is the conductance G_{eq}, representing dielectric losses in the fluid between the inner and outer conductor of the stub resonator. The value of G_{eq} can now be determined from the A–f plot obtained with the resonator filled with fluid and using Eqs. (16)–(18).

Finally, the dielectric loss tangent at resonance, describing the phase angle between the lumped element capacitor voltage and capacitor current is given by Eq. (19):

$$\tan\delta = \frac{G_{eq}}{\omega \cdot C_{eq}} \tag{19}$$

Once the values of R_{eq} and G_{eq} have been determined, all parameters in Eqs. (2)–(11) are known. As a result, the A–f plot can be simulated and compared to the one experimentally obtained.

3. Experimental

The experiments were performed with a HAMEG HMS3010 3 GHz Spectrum Analyzer with Tracking Generator, both with an internal resistance Z_s of 50 Ω. In order to check the internal resistance of the function generator, its output amplitude was measured with a high impedance oscilloscope to amount 1.34 V. Subsequently, the output was loaded with a 50 Ω resistor, resulting in output amplitude of 0.67 V. This result proves that the internal resistance of the internal frequency generator of the spectrum analyzer is indeed very close to 50 Ω. The interconnecting transmission lines have characteristic impedance Z_0 of 50 Ω.

For the experiments, two types of coaxial resonators were designed: a batch resonator and a flow-through resonator. Apart from the (in) ability of flowing through the measured solutions, both coaxial resonators are essentially of the same design but with different dimensions, as summarized in Table 1. When filled with the same dielectric solution and according to Eq. (1), both types of resonators have a different resonant frequency.

Both inner and outer conductors are made of copper. The transmission lines were connected to the resonator by using SMA (SubMiniature version A) connectors with a total length of 6 mm.

To investigate the performance of both types of resonators, the following solutions were tested as dielectric between inner and outer conductor: demineralized water with a conductivity of 1×10^{-4} S/m, ethanol (100% denatured with 2-propanol 2.5%) supplied by BOOM B.V., glycerol (100%) supplied by VNR.

In order to prevent undesired reflections of electromagnetic waves at the transmission line interfaces, ideally all components of the system should have the same characteristic impedance. The characteristic impedance of the coaxial stub resonator equals (20):

$$Z_0 = \frac{1}{2\pi}\sqrt{\frac{\mu_0\mu_r}{\varepsilon_0\varepsilon_r}}\ln\left(\frac{D}{d}\right) \tag{20}$$

The characteristic impedance of both resonators as calculated with Eq. (20) was 39.8 Ω for water, 72.3 Ω for ethanol and 55.5 Ω for glycerol. An inevitable consequence, and hence accepted compromise, of the range of characteristic impedance of the different solutions used (39.8–72.3 Ω) is that the resonator was not perfectly matched to the function generator, spectrum analyzer and transmission lines, all with an impedance of 50 Ω.

Experiments were performed at 20 °C and repeated 11 times. From the base frequency obtained for each experiment, the relative dielectric permittivity ε_r was calculated using Eq. (1). Subsequently, the mean value of ε_r was calculated for the set of 11 experiments. The experiments in the flow-through resonator were executed at recycling conditions, i.e., by pumping the liquid under investigation from a 5 l container through the vertically positioned resonator in bottom-to-top direction and with the outflow returning into the feed container. In order to deal with the relatively high viscosity of glycerol, a Master flex peristaltic pump, model 77200-60 was used for this purpose.

It is noted that over time and depending on the dielectric and the process conditions, both the inner conductor and the outer conductor of the flow-through resonator may be covered by a thin layer of metal oxide. This effect was observed when the flow-through resonator was operated continuously with a copper inner conductor for a period of 1 month when filled with drinking water. In that particular case the resonator can be considered to be constructed with two concentric dielectrics: one dielectric of metal oxide around the inner conductor and the dielectric under investigation. It appears that, in this particular case, the small layer of metal oxide dielectric around the inner conductor may have a significant influence on the effective dielectric permittivity, i.e., on the resonant frequency of the coaxial resonator. This problem can be solved by isolating the inner conductor with a thin inert coating and by correcting for the influence of this coating on the resonant frequency. Prior to all experiments reported in this contribution, both inner and outer conductors of the coaxial resonators were inspected to ensure that neither of them was coated by a small layer of metal oxide.

In order to check whether the measurements are influenced by coupling or radiation effects, the experimental set-up was placed in a Faraday cage with a characteristic size of 70.0 cm and a wall thickness of 3.0 mm. Based on a coaxial stub of 34.0 cm length, filled with demineralized water as dielectric, results were compared to those obtained without using a Faraday cage. It was found that, within experimental error, application of a Faraday cage did not result in a frequency shift whereas the difference in amplitude at the base frequency amounted to less than 4%. We therefore concluded that under the laboratory conditions applied measurements were free of environmental interferences.

4. Results and discussion

Fig. 5 shows the A–f plot for water, ethanol and glycerol as obtained with the batch resonator and the experimental set-up in Fig. 1.

Substitution of the obtained base resonant frequencies (24.8 MHz for water, 44.1 MHz for ethanol and 33.9 MHz for glycerol) into Eq. (1) results in dielectric permittivity values of re: $\varepsilon_{water} = 80.2 \pm 0.9$ (78.76 (79.5) according to [32]), $\varepsilon_{ethanol} = 25.4 \pm 0.3$ (24.35 (25.13) according to [32]) and $\varepsilon_{glycerol} = 41.8 \pm 0.8$ (42.49) according to [32], with reported literature values given in between brackets. These results thus reveal

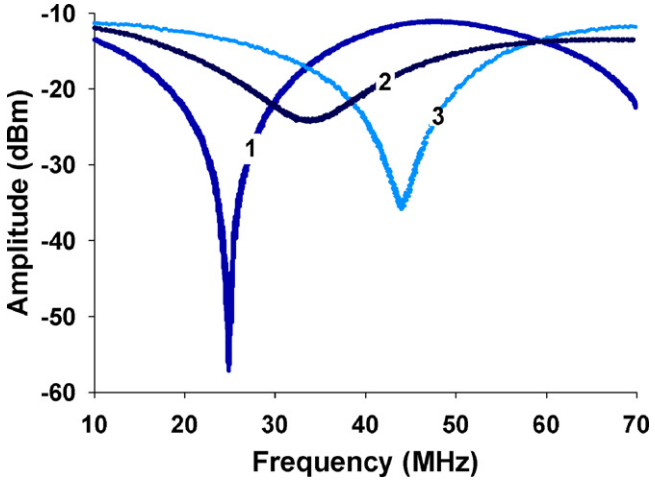

Fig. 5. Amplitude versus frequency plot for demineralized water (1), glycerol (2) and ethanol (3) as obtained with the batch resonator and the experimental set-up in Fig. 1. All experiments were executed at 20 °C.

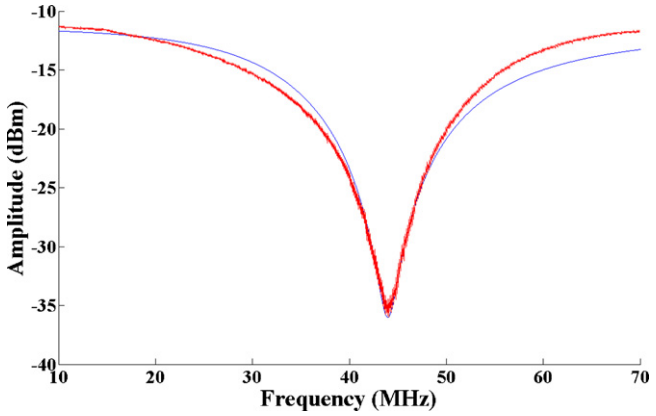

Fig. 6. Amplitude versus frequency plot for experimental data of ethanol (blue) and modeling (red) for the batch resonator using Eqs. (3)–(13) and the parameters in Table 2. (For interpretation of the references to color in this figure legend, the reader is referred to the web version of the article.)

that the batch resonator performs well with water, ethanol and glycerol as dielectrics. Resonance in all *A*–*f* plots showed up as a minimum at a frequency predicted by reported values obtained with different experimental methods. We, therefore, conclude that it is technically feasible to determine the dielectric permittivity of a liquid by using this batch resonator.

As mentioned in the sensing technique section, the shape of the *A*–*f* plots in Fig. 5 are mainly determined by the skin effect in inner and outer conductors of the coaxial stub resonator and by dielectric losses in the fluid between them. The *A*–*f* plot of ethanol will further be investigated using the lumped element model described in Section 2. In order to quantify the skin effect, i.e., the value of R_{eq}, a coaxial stub resonator with a length of 1.70 m was constructed. The other characteristic dimensions of the stub resonator, such as construction material, diameter of the inner and outer conductors were identical to those listed in Table 1. Air was applied as dielectric between inner and outer conductor. The length of the coaxial stub resonator was chosen as such that its resonant frequency with air as dielectric was about 44 MHz, i.e., approximately the same as the resonant frequency of the smaller stub resonator filled with ethanol. Since the 1.70 m coaxial stub was filled with dry air, the dielectric losses in the stub were negligible so that $G_{eq} = 0$. The values for the voltage input of the function generator V_{in} and the recorded voltage by the spectrum analyzer V_{out} at the resonant frequency of the 1.70 m coaxial stub resonator were measured to amount 66.83 mV and 2.51 mV respectively, see also Table 2. Substitution of these values in Eq. (18) provides a R_{eq} value of 0.98 Ω. Since the coaxial stub resonator applied for the experiments with ethanol has a length of 34 cm, see also Table 2, its value of R_{eq}, i.e., $R_{eq(fluid)}$, is smaller than that of the 1.70 m stub resonator filled with air. Substitution of these values in Eq. (17) results in $R_{eq(fluid)} = 0.20$ Ω at the resonant frequency of 44 MHz. Since $R_{eq(fluid)}$ is known, the value of G_{eq}, representing the dielectric loss in the fluid, can now be calculated from the attenuation at the resonant frequency of 44 MHz for the 0.34 m coaxial stub resonator filled with ethanol. The values for the voltage input of the function generator V_{in} and the recorded voltage by the spectrum analyzer V_{out} at the resonant frequency of the 0.34 m coaxial stub resonator filled with ethanol were measured to amount 60.74 mV and 3.55 mV respectively. Substitution of the determined values for V_{in}, V_{out} and R_{eq} in Eqs. (16)–(18) provides the value for $G_{eq} = 1.07 \times 10^{-3}$ S. Substitution of this value into Eq. (19) provides the dielectric loss tangent: $\tan\delta = 0.04$.

Once all parameters defining the *A*–*f* plot with the use of Eqs. (3)–(11) have been determined, an *A*–*f* plot for the lumped element circuit in Fig. 3 can be calculated and compared to the experimentally determined one. The result is show in Fig. 6. The simulations were executed by the use of MATLAB 7.9.0 (R2009b) software.

Fig. 6 reveals a good agreement between the simulated and experimentally determined *A*–*f* plots. Hence, it is concluded that the open ended quarter wave length batch coaxial stub resonator performs as expected and that the lumped element circuit in Fig. 3 describes the behavior of the coaxial stub resonator well near its base resonant frequency.

Fig. 7 shows an *A*–*f* plot for water as obtained with the batch resonator but now over a broader frequency range as compared to Fig. 5, i.e., for a frequency range from 10 to 150 MHz.

Fig. 7 shows that apart from the base frequency (or 1st harmonic); the batch resonator detects the higher harmonics also. The dielectric permittivity of demineralized water as calculated from the first, second and third harmonic in Fig. 7 are 80.2 ± 0.89, 79.4 ± 0.51 and 78.9 ± 0.54, respectively. The decline in amplitude of the signal with increasing frequency can be explained by an increase of energy loss mainly as a result of the decreasing penetration depth of the current in the inner and outer conductors due to an increased skin effect with increasing frequency.We also tested the flow-through resonator and Fig. 8 shows amplitude versus frequency plot for water, ethanol and glycerol.

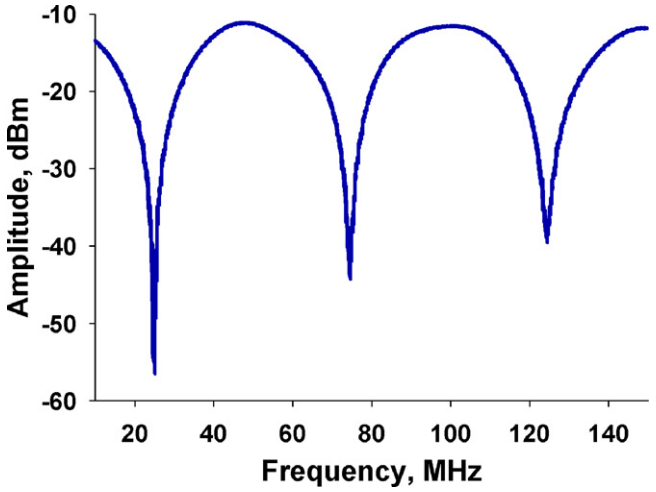

Fig. 7. Amplitude versus frequency plot for demineralized water obtained with the batch resonator at 20 °C. Resonant frequencies for the first, second and third harmonics are 24.8 MHz, 74.3 MHz and 124.7 MHz respectively.

Table 2
Measurements with a 1.70 m quarter wavelength coaxial stub resonator with air as dielectric and with a 0.34 m quarter wavelength coaxial stub resonator filled with ethanol in order to asses the values for R_{eq} and G_{eq} representing losses as a result of the skin effect and dielectric losses respectively.

Dielectric	Input amplitude (dBm)	Resonance amplitude (dBm)	V_{in} (mV)	V_{out} (mV)	R_{tot} (Ω)	R_{eq} (Ω)	L_{eq} (H)	C_{eq} (F)	G_{eq} (S)	tgδ
Air	10.5	39	66.83	2.51	0.98	0.98	6.43E−07	2.02E−11	0	
Ethanol	11.33	36	60.74	3.55	1.55	0.20	1.29E−07	1.01E−10	1.07E−03	0.04

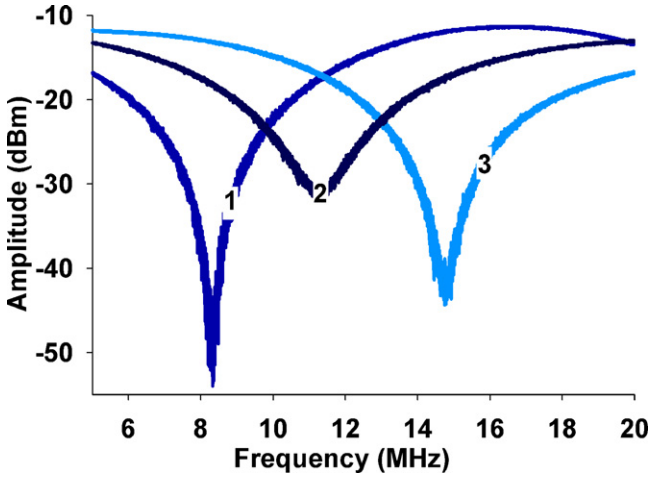

Fig. 8. Amplitude versus frequency plot for demineralized water (1), glycerol (2) and ethanol (3) as obtained with the flow-through resonator and the experimental set-up in Fig. 1. All experiments were executed at 20 °C.

Compared to Fig. 5, obtained with the batch resonator, results are very similar. Substitution of the resonant frequencies determined from Fig. 8 in Eq. (1) results in the following dielectric permittivity values of water, ethanol and of glycerol: $\varepsilon_{water} = 79.9 \pm 0.86$ (78.76 (79.5) according to [32]), $\varepsilon_{ethanol} = 24.2 \pm 0.50$ (24.35 (25.13) according to [32]) and $\varepsilon_{glycerol} = 42.9 \pm 0.56$ (42.49) according to [32]). We conclude that the flow-through resonator performs well with the solutions tested because obtained values are close to reported experimental values by others (given in between brackets).

Fig. 9 shows an *A–f* plot for water as obtained with the flow through resonator but now over a broader frequency range as compared to Fig. 8, i.e., for a frequency range from about 5 to 150 MHz.

As observed with the batch resonator, the flow through resonator is also able to reveal the higher harmonics. When calculating the dielectric permittivity of demineralized water from the first, second and third harmonic, we render values of 79.9 ± 0.86, 78.7 ± 1.5 and 78.9 ± 1.2, respectively.

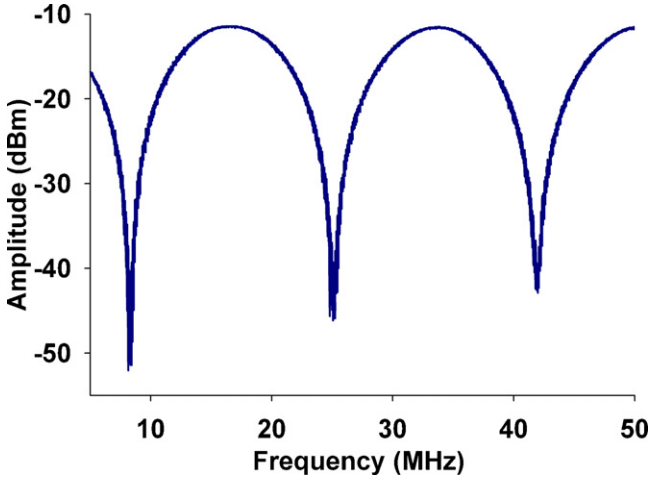

Fig. 9. Amplitude versus frequency plot for demineralized water obtained with the flow-through resonator at 20 °C. Resonance frequency for the first, second and third harmonics are 8.3 MHz, 25.07 MHz, 41.99 MHz, respectively.

An important characteristic of our coaxial stub is that resonance occurs at relative low frequencies. By implication, the use of commercially available but relatively expensive spectrum or network analyzers to delineate responses in the high frequency range is no longer required. Obviously, this reduces the investment costs for application substantially.

As was remarked already, not only the resonant frequencies but also the shape of the amplitude versus frequency curves contains information on the dielectric properties of the samples. In case dielectric losses in the sample are high, the quality factor of the coaxial resonator will decrease. In addition, the amplitude versus frequency plot will be affected by imperfections in the experimental set-up. It is expected that more detailed modeling of the resonator will guide us to gain more understanding of the system described here as well as the dielectric properties of fluids under investigation.

5. Conclusions

- The concept of a quarter wave length open-ended coaxial stub resonator as sensing device was successfully applied to measure the dielectric permittivity of water, ethanol and glycerol.
- The coaxial resonator presented in this study performs well both in the batch as in the flow-through mode of operation.
- The flow-through mode of operation allows the continuously online monitoring of fluid samples.
- It is expected that the coaxial resonator concept can be developed further into a cost-efficient and low maintenance sensor for dielectric spectroscopy in a broad field of specific applications.

6. Future steps

Based on the results presented in this study, we expect that the concept of the coaxial stub resonator as sensing device proves useful in a wide range of applications. Examples include the detection of (very early) corrosion or biofouling on the inner conductor surface of the coaxial stub, quality control in the food industry (e.g., milk, soft and alcoholic drinks) and measuring the load and/or saturation level of ion exchange resins and activated carbon applied as dielectrics in a coaxial stub-based device.

In addition, miniaturization of the coaxial stub sensor allows the application of much higher frequencies, i.e., frequencies in the GHz range. This, in turn, broadens the application range significantly as it gives way to complex dielectric radio-frequency spectroscopy for the detection of, for instance, molecular structures, micelles or micro organisms in liquid samples.

Acknowledgements

This work was performed in the TTIW-cooperation framework of Wetsus, Center of Excellence for Sustainable Water Technology (www.wetsus.nl). Wetsus is funded by the Dutch Ministry of Economic Affairs, the European Union Regional Development Fund, the Province of Fryslân, the City of Leeuwarden and the EZ/Kompas

program of the "Samenwerkingsverband Noord-Nederland". The authors thank the participants of the research theme Sensoring for the fruitful discussions and their financial support.

Furthermore, the authors wish to thank Prof. Dr. Ir. F.B.J. (Frank) Leferink for his large scientific contribution to this work.

References

[1] A. Fabbri, T. Fen-Chong, O. Coussy, Dielectric capacity, liquid water content, and pore structure of thawing–freezing materials, Regions Science and Technology 44 (January (1)) (2006) 52–66.
[2] H. Eller, A. Denoth, A capacitive soil moisture sensor, Journal of Hydrology 185 (November (1–4)) (1996) 137–146.
[3] F. Kizito, C.S. Campbell, G.S. Campbell, D.R. Cobos, B.L. Teare, B. Carter, J.W. Hopmans, Frequency, electrical conductivity and temperature analysis of a low-cost capacitance soil moisture sensor, Journal of Hydrology 352 (May (3–4)) (2008) 367–378.
[4] T. Fen-Chong, A. Fabbri, J.-P. Guilbaud, O. Coussy, Determination of liquid water content and dielectric constant in porous media by the capacitive method, Comptes Rendus Mecanique 332 (August (8)) (2004) 639–645.
[5] U.C. Hasar, M.T. Yurtcan, A microwave method based on amplitude-only reflection measurements for permittivity determination of low-loss materials, Measurement 43 (November (9)) (2010) 1255–1265.
[6] A. García, J.L. Torres, E. Prieto, M. De Blas, Dielectric properties of grape juice at 0.2 and 3 GHz, Journal of Food Engineering 48 (May (3)) (2001) 203–211.
[7] F.N. Dalton, M.Th. Van Genuchten, The time-domain reflectometry method for measuring soil water content and salinity, Geoderma 38 (September (1–4)) (1986) 237–250.
[8] D.M. Hagl, D. Popovic, S.C. Hagness, J.H. Booske, M. Okoniewski, Sensing volume of open-ended coaxial probes for dielectric characterization of breast tissue at microwave frequencies, IEEE Transactions on Microwave Theory and Techniques 51 (April (4)) (2003) 1194–1206, doi:10.1109/TMTT.2003.809626.
[9] Y. Wang, M.N. Afsar, Measurement of complex permittivity of liquids using waveguide techniques, Progress in Electromagnetics Research 42 (2003) 131–142.
[10] V.V. Komarov, S. Wang, J. Tang, Permittivity and Measurements, vol. 4, Wiley Encyclopedia of RF and Microwave Engineering, 2005, pp. 3693–3711.
[11] I. Ciofi, M.R. Baklanov, Z. Tőkei, G.P. Beyer, Capacitance measurements and *k*-value extractions of low-*k* films, Microelectronic Engineering 87 (November (11)) (2010) 2391–2406.
[12] U. Kaatze, V. Uhlendorf, Zeitschrift Fur Physikalische Chemie Neue Folge 126 (1981).
[13] J. Baker-Jarvis, M.D. Janezic, P.D. Domich, R.G. Geyer, Analysis of an open-ended coaxial probe with lift-off for nondestructive testing, IEEE Transactions on Instrumentation and Measurement 43 (October (5)) (1994) 711–718.
[14] J. Sheen, Study of microwave dielectric properties measurements by various resonance techniques, Measurement 37 (March (2)) (2005) 123–130.
[15] M.S. Venkatesh, G.S.V. Raghavan, An overview of dielectric properties measuring techniques, Canadian Biosystems Engineering 47 (2005), 15-7.30.
[16] M.V. Storey, B. van der Gaag, B.P. Burns, Advances in on-line drinking water quality monitoring and early warning systems, Water Research 45 (January (2)) (2011) 741–747.
[17] D. Singwong, N. Siripon, A wide-band bandpass filter using a novel embedded short-circuited stub resonator, in: Microwave Conference Proceedings (APMC), 2010, Asia-Pacific, March, 2011, pp. 1086–1089.
[18] G.H. Huff, S. Goldberger, A coaxial stub microfluidic impedance transformer (COSMIX), IEEE Microwave and Wireless components Letters 20 (March) (2010).
[19] J. Lamb, The experimental behaviour of the coaxial line stub, electrical engineers – Part III: Radio and communication engineering, Journal of the Institution of Electrical Engineers 93 (May (23)) (1946) 188–190.
[20] J. Carroll, M. Li, K. Chang, New technique to measure transmission line attenuation, IEEE Transactions on Microwave Theory and Techniques 33 (January) (1995).
[21] J.M. Drozd, W.T. Joines, A capacitively loaded half-wavelength tapped-stub resonator, IEEE Transactions on Microwave Theory and Techniques 45 (July) (1997).
[22] Y.-H. Chou, M.-J. Jeng, Y.-H. Lee, Y.-G. Jan, Measurement of RF PCB dielectric properties and losses, Progress in Electromagnetics Research Letters 4 (2008) 139–148.
[23] H. Heck, Module 5: Advanced Transmission Lines Topic 5: 2 Port Networks & S-Parameters, OGI EE564, 2008, http://home.comcast.net/~howard.heck/.
[24] D.M. Pozar, Microwave Engineering, Addison Wesley Publishing Company, 1993, ISBN 0-201-50418-9.
[25] O. Zinke, H. Brunswig, Hochfrequenztechnik 1, Hochfrequenzfilter, Leitungen, Antennen, 6. Auflage, Springer, Berlin, 2000, pp. 86–88.
[26] D.M. Pozar, Microwave Engineering, Wiley, 2004.
[27] R.E. Collin, Foundations for Microwave Engineering, Wiley IEEE, 2000.
[28] F. Leferink, C. Roeloffzen, Handout Transmission Media: Transmission Lines, University of Twente, 2007.
[29] S.M. Xu, B. Bo, Z. Klimek, Andrew, The research on lumped parameter equivalent circuit of transmission line, in: 8th International Conference on Advances in Power System Control, Operation and Management (APSCOM 2009), November, 2009, pp. 1–5.
[30] A. Niknejad, Lossy Transmission Lines and the Smith Chart, University of California, Berkeley, Course EECS 117, Lecture 6, http://rfic.eecs.berkeley.edu/~niknejad/ee117/pdf/lecture6.pdf.
[31] O. Coufal, Inductance of coaxial cable, Energyspectrum 3 (1) (2008) 1–5.
[32] C. Wohlfarth, M.D. Lechner, Static Dielectric Constants of Pure Liquids and Binary Liquid Mixtures, Supplement to IV/6, Series: Landolt-Börnstein: Numerical Data and Functional Relationships in Science and Technology – New Series, vol. 17, Subseries: Physical Chemistry, 2008, p. 203.

Biographies

Natalia A. Hoog-Antonyuk studied and received her Engineer Diploma within specialization "Organization and Technology of Information Security", at Tomsk State University of Control Systems and Radioelectronics (TSUCSR), Russia in 2002. After she worked as an engineer and an assistant in the Department of Radioelectronics and Data Protection, (TSUCSR), at the same time, she was a member of international project The Netherlands (TU Delft)-Russian (TSUCSR) with research activities in the area of advanced Ground-Penetrating Radar (GPR) technology. At present time, she is PhD in the Laboratory of Biosensors, the Lab-on-a-Chip group, part of the MESA+ Research Institute, of the University of Twente and a researcher at Wetsus, center of excellence for sustainable water technology, the Netherlands.

Wouter Olthuis received his MSc degree in electrical engineering from the University of Twente, Enschede, The Netherlands in 1986. In that year, he joined the Center for MicroElectronics, Enschede (CME). In 1987 he started his PhD project and received the PhD degree from the Biomedical Engineering Division of the Faculty of Electrical Engineering, University of Twente, in 1990. Since 1991 he has been working as an Assistant Professor in the Laboratory of Biosensors, part of the MESA+ Research Institute, of the University of Twente and as such co-supervising many projects on both physical and (bio)chemical sensors and sensor systems for medical and environmental applications. Currently, he is Associate Professor in the BIOS Lab-on-Chip group of the MESA+ Institute of Nanotechnology and is as such responsible for the theme Electrochemical sensors and Sensor systems. Since 2006 he is also the Director of the Educational Programme of Electrical Engineering at the Faculty of Electrical Engineering, Mathematics and Computer Science at the University of Twente.

Mateo J.J. Mayer studied chemical engineering at Eindhoven University of Technology, The Netherlands and received his PhD in 1995 on the project titled "The dynamics of batch and continuous emulsion polymerization". From 1995 to 2006 he worked for Akzo Nobel at different R&D positions, as strategy analyst of Akzo Nobel Salt and as innovation manager of Akzo Nobel Base Chemicals. In 2007 he started at Wetsus, a research institute in the field of water technology, as a scientific project manager in the fields of sensoring and advanced waste water treatment. At the same time he founded EasyMeasure B.V., a start-up company focusing on the development of new technological concepts. In 2009 and 2010 he was co-founder of 4 spin-off start-up companies and at present he is technical director of these companies.

Doekle Yntema received his MSc in Electrical Engineering in 2004 and his PhD in 2008 both at the University of Twente, The Netherlands. The subject of his research was mainly focused on Micromechanics (MEMS) and acoustics. During this time he was closely involved in the startup of a company developing acoustic flow sensors. After his PhD he worked as a post-doc at the MESA+ institute and designed a miniature microphone capable of operating at very high temperatures. In 2010 he decided to move to Wetsus where he first worked as a post-doc and later as scientific project leader.

Henk Miedema studied a combination of biology and biochemistry at the University of Groningen, The Netherlands, where he also earned a PhD in electrophysiology in 1992. After that he occupied several post-doc positions in Amsterdam, Montreal, Cuernavaca (Mexico) and Cambridge (UK). The central theme during these years of post-doc research was (the mechanism of) ion transport across biological membranes. In 2002 he returned to The Netherlands to become researcher at Biomade, a spin-off of the University of Groningen. In 2008 he started working as project leader for Wetsus, a Research Institute in the field of Water Technology. His current research interests include sensors for water composition and ion selective membranes.

Albert van den Berg received his MSc in applied physics in 1983, and his PhD in 1988 both at the University of Twente, the Netherlands. From 1988 to 1993 he worked in Neuchatel, Switzerland, at the CSEM and the University (IMT) on miniaturized chemical sensors. From 1993 until 1999 he was research director Micro Total Analysis Systems (μTAS) at MESA, University of Twente. In 1998 he was appointed as part-time professor "Biochemical Analysis Systems", and later in 2000 as full professor on Miniaturized Systems for (Bio)Chemical Analysis in the faculty of Electrical Engineering. He received several honors and awards such as Simon Stevin (2002), ERC advanced grant (2008), Spinoza prize (1009) and honorary university professorship (2010). He has co-authored over 220 papers (H = 36) and over 10 patents, and has been involved in >5 spin-off companies. His current research interests focus on microanalysis systems and nanosensors, nanofluidics and single cells and tissues on chips, especially with applications in personalized health care and development of sustainable (nano) technologies.